
Article:
Krueger, H., Fletcher, D. orcid.org/0000-0002-1562-4655 and Cruden, A. (2021) Vehicle-to-Grid (V2G) as line-side energy storage for support of DC-powered electric railway systems. Journal of Rail Transport Planning & Management, 19. 100263. ISSN 2210-9706

https://doi.org/10.1016/j.jrtpm.2021.100263

Vehicle-to-Grid (V2G) as line-side energy storage for support of DC-powered electric railway systems

Hannes Krueger [a,*], David Fletcher [b], Andrew Cruden [a]

[a] *EPSRC Centre for Doctoral Training in Energy Storage and its Applications, University of Southampton, Southampton, United Kingdom*

[b] *University of Sheffield, Department of Mechanical Engineering, Sheffield, United Kingdom*

* *Corresponding author*

Abstract: Two predominant areas of ongoing transport electrification are the uptake of electric vehicles (EVs) in personal transportation and electrically powered trains for mass transportation - both significantly increase demand stresses on the electric power grid. In this research, a novel V2G application to support electrically powered rail transport is proposed. A local V2G network can reduce peak demand stresses on the power grid arising from electrified rail traffic and enable brake energy recovery from DC-powered electric trains. A case study examining an existing third- rail DC-powered rail system in England supported by a simulated population of aggregated parked EVs is presented. Simulation results for 24 h of V2G supported rail traffic from the view of a single train station with nearby V2G enabled car park are discussed. Therein the EV population size, charging rate limits per EV and the overall power made available from the power grid are variables. The V2G network's ability to absorb power from regenerative braking on the rail system was found to be more sensitive to changes in EV charging rates than its ability to provide traction power. In particular, careful power management is required to avoid charging EVs 'too quickly' during periods without rail traffic.

Keywords: Vehicle-to-Grid; Aggregator control; Electrified rail; Peak demand reduction; Line-side energy storage

1. Introduction

The transportation sector is responsible for much of the global energy consumption, accounting for around 36% of all energy consumption among member states of the International Energy Agency (IEA) (International Energy Agency, 2019a). Global ambitions of decarbonisation and a reduced dependency on fossil fuels are thus heavily targeted at the transport sector – largely through transport electrification. Electrification affects both individual and mass transportation and requires ongoing infrastructure upgrades in both areas for electric power grids to cope with the increased electricity demands. For individual transport, increased electro-mobility manifests itself as an ever-growing number of EVs on the streets worldwide. The global EV fleet grew by 2 million in 2018 alone, exceeding 5.1 million (including plug-in hybrid electric vehicles) (International Energy Agency, 2019b).

While the emergence of EVs also affects public transport, sometimes in the form of electrically driven busses (Li et al., 2018), electrification of mass transport is dominated by railway electrification. As electrically driven trains are typically continuously powered by either overhead transmission lines or third rail and fourth rail systems, even electrifying existing railways (for example replacing diesel locomotives) requires significant investments in local power infrastructure. Transport electrification also poses challenges to the wider electric power grid. The shift away from fossil fuel combustion increases the total electricity demand and uncontrolled charging of an ever-increasing number of EVs creates power demand peaks that risk overwhelming local distribution networks (EA technology, 2018). The risk of overloading substations is particularly severe when the peak power demand from EV charging coincides with the megawatt-scale power demands of electric rail vehicles (Grenier and Page, 2012).

It is noteworthy that transport electrification is by no means the only considerable transformation of our electricity systems. Instead, it is accompanied by significant shifts towards renewable electricity generation. As a result, increased electricity consumption from electro-mobility coincides with increased intermittency in the electricity supply. Attempts to mitigate any issues surrounding electricity supply intermittency typically involves energy storage technologies (Kim et al., 2017). Electric rail systems as large-scale power consumers may also employ energy storage as a means of demand-side control. Here, energy storage may help reducing peak power demand stresses on the power grid that arise from the traction power demands of electric trains – particularly during acceleration where traction power demand may reach several megawatts depending on the rail system. This traction power could be fully or partially supplied through local energy storage, thus reducing stress on the electric power grid.

Another area in which energy storage can be beneficial is train brake energy recovery; in particular for DC-powered networks. For rail systems with AC power supplies (typically operating at ~25 kV), electricity from regenerative braking can usually be fed back into the power grid without major transmission losses. DC networks, however, typically operate at much lower voltages (~650–1500 V) significantly lowering the efficiency of power transmission. Thus regeneration of power from brake energy recovery into the grid is not currently a common feature of DC-powered networks and rail networks using third rail, fourth rail or overhead catenary DC power supply may benefit from energy storage enabling effective regenerative braking.

Unlike approaches such as dwell time optimisation (Lin et al., 2016), in which power from regenerative braking of one train is immediately absorbed as traction power by another, the usage of energy storage does not interfere with train schedules. Various types of energy storage, such as batteries or supercapacitors, have been proposed either on-board or along track lines to accept power from regenerative braking for later use during acceleration (Ceraolo et al., 2018). On-board solutions may offer additional benefits such as partial independence from any power supplying infrastructure along the track (Mwambeleko and Kulworawanichpong, 2017), thus allowing electric rail vehicles to travel on non-electrified track sections – although at the cost of increased weight per vehicle, additional maintenance requirements and per-unit costs.

In this work, an alternative energy storage solution is proposed: a V2G network in proximity to an electric rail system. V2G is an energy storage concept in which the battery packs of parked road EVs are aggregated and charged or discharged to provide a variety of grid services (Tomić and Kempton, 2007). Typical grid services for V2G include frequency regulation (maintaining the grid frequency at 50 or 60 Hz, depending on region) (Peng et al., 2017), acting as a pseudo-spinning reserve (Pavić et al., 2015) or load balancing (discharging EVs at periods of peak stresses on the grid and charging at low demand periods) (Habib et al., 2015). In the system proposed here, the V2G network acts as a buffer between the power grid and the electric rail system, as shown in Fig. 1.

Unlike other energy storage technologies, V2G utilises already existing storage that would otherwise lay dormant (batteries of parked EVs). Instead of manufacturing and maintaining dedicated energy storage systems for electric rails systems, existing EV batteries are bestowed with a secondary purpose. When combined with smart charging technologies, EVs could be turned from a burdensome load on the power grid, into a valuable tool for maintaining grid stability. The main disadvantage of V2G compared to other energy storage solutions is the reliance on the availability of EVs in sufficient numbers. This work provides an initial investigation into the scale of the required EV population.

The aggregated EV population may be discharged to provide traction power to nearby accelerating trains (reducing peak demand stresses on the grid) or charged to absorb power from (and thus enabling) trains' regenerative braking. In the absence of nearby rail vehicles, the EV population may use the shared connection to the power grid for charging

purposes. Additional charging cycles from V2G participation can accelerate the degradation of connected EV batteries (Darcovich et al., 2017). Costs associated with battery degradation pose a financial risk to EV owners requiring fair compensation for the usage of EVs in a V2G network (Freeman et al., 2017). The compensation of EV owners should not only cover costs incurred but also create a profit motive to encourage V2G participation.

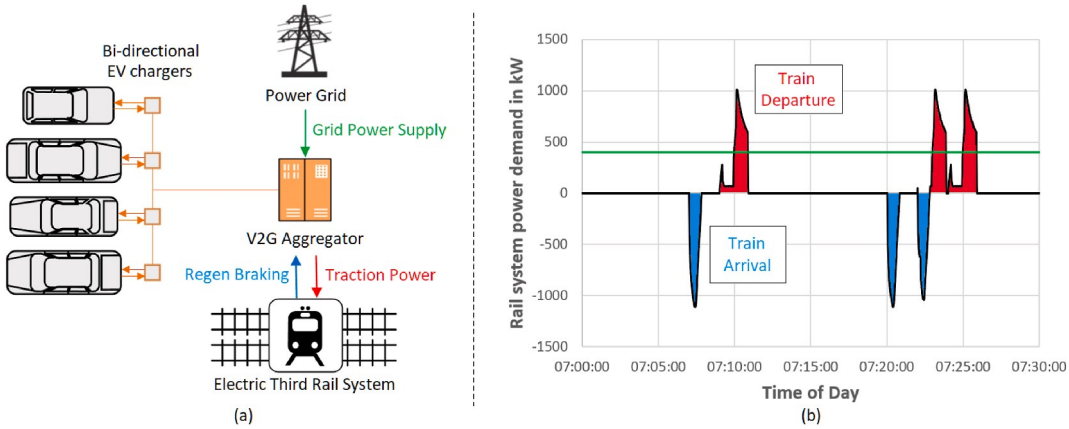

Fig. 1. (a) System overview and power flows: aggregated EV population acts as a buffer between the grid connection and the fluctuating rail system power demands to ensure steady power flow from the grid (Krueger and Cruden, 2020a); (b) Rail system power demand over 30 min: traction power drawn for train acceleration - positive/red, power supplied from regenerative braking - negative/blue.

2. Rail system power demand model

The Merseyrail 750 V third rail powered DC rail network serves as a case study for this work (Stewart et al., 2011), in particular, the Hoylake train station on the 'Wirral Line'. Hoylake itself is interesting as the train station and the single substation powering this section of the rail network are in very close proximity (Fletcher et al., 2020) (thus removing the need to analyse interactions between multiple substations or transmission losses). The train station has two tracks and only serves this line (both directions). At the time considered this section of the Merseyrail network did not utilise regenerative braking and operated exclusively British Rail Class 507/508 trains.

The power consumption of trains moving along the whole line has been modelled in detail and validated in the previous work of one of this paper's authors (Fletcher et al., 2020). Besides describing the traction power requirements of trains moving on the rail network, the theoretical usage of regenerative braking has also been included. Parts of this existing model forms the basis of this work: the power demand profile of a single train accelerating from a standstill at 'West Kirby' train station and stopping at Hoylake. The track section Hoylake-West Kirby is single-ended (West Kirby is at the end of the 'Wirral Line') and thus fully powered by the substation at Hoylake. The speed profile of the train and the corresponding power demand curve (negative demand represents power from regenerative braking) are shown in Fig. 2 (a) and 2 (b) respectively.

The power demand profile has been separated into two distinct 'events' (as required by the V2G aggregator control, see section 4): a train departure event (acceleration from standstill, slow speed movement close to the station, then to travelling speed, traction power required) and a train arrival event (deceleration from travelling speed to standstill, energy from regenerative braking needs to be dissipated).

To construct a 24-h rail system power demand profile for Hoylake train station these events were matched with each departure on the Hoylake train schedule (Merseyrail, 2019) (both directions, for weekdays, December 2019 to May 2020) under the following simplifying assumptions: 1) train arrivals and departures at/from Hoylake follow the same

speed profile as the modelled train in both directions. 2) every train follows the same speed profile ('human factors', i.e. differences due to driver behaviour is not considered). 3) each train scheduled departs perfectly on time after a minimum dwell time of 60 s 4) no rail traffic not listed on the public schedule (neither stopping at nor 'passing through' Hoylake).

It should be noted that this creates a highly idealised power demand profile. It does not capture any potential deviations that would be expected between train journeys in normal rail operation (e.g. differences in vehicle weight due to passenger numbers or driver behaviour may alter power demands). Neither is any potential overlap of train arrival and train departure events considered (which should not occur if the public train schedule is strictly adhered to). A V2G network supporting these variable power demands needs to be resilient and dynamically adjust to any such deviations (achieved here through V2G aggregator control combining predictive and reactive scheduling techniques, see section 4 and (Krueger and Cruden, 2020a)). The resulting 24-h power demand model used in the following discussion features 117 train departures (see Fig. 3). As such, slight deviations from the idealised power demand profile for individual events would not significantly alter the findings presented in section 4 onwards.

For about 3.6 h (~15% of the day) the rail system requires traction power for acceleration while regenerative braking could generate power for about 1.5 h per day (~6%) – during these times the rail system could benefit from a connected V2G network. The rest of the day – about 18.9 h – no rail traffic is present (EVs on the V2G network could charge freely during these periods). Each train departure event has an energy consumption of roughly 46 MJ or ~12.7 kWh. Over 24 h, this adds up to about 5382 MJ or ~1486 kWh. Similarly, each arrival event could regenerate 35 MJ or ~9.7 kWh, adding up to about 4095 MJ or ~1135 kWh per day. If this regenerative braking energy could be fully 'saved', the accumulative energy savings would be equivalent to the electricity consumption of about 115 UK households (based on an average per household electricity consumption of about 3600 kWh per year, as of 2018 (Department for Business, Energy & Industrial Strategy, 2019)). At a typical electricity price of 15p per kWh, this is equivalent to savings of about £62,000 in electricity costs.

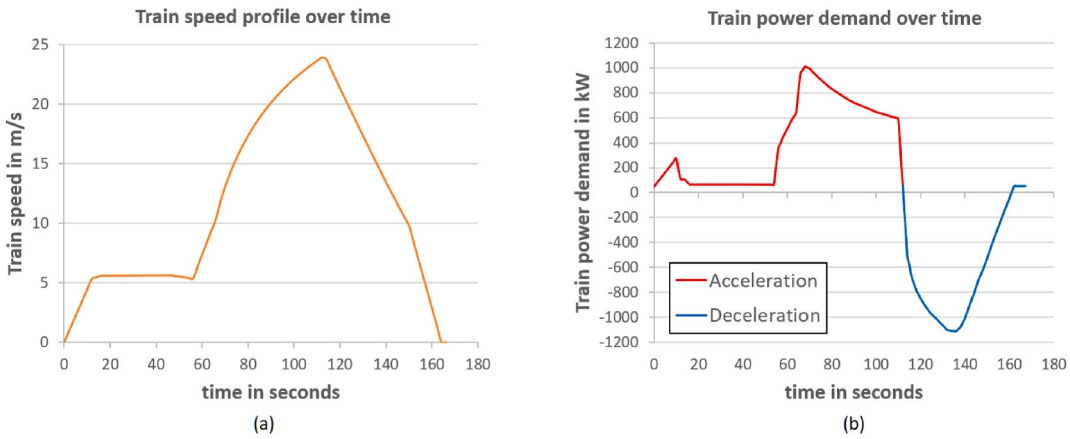

Fig. 2. (a) Assumed speed profile of simulated train (based on GPS data captured during real-life train journey); (b) Resulting train traction power demand (as experienced by the substation) during acceleration and regen power output during deceleration.

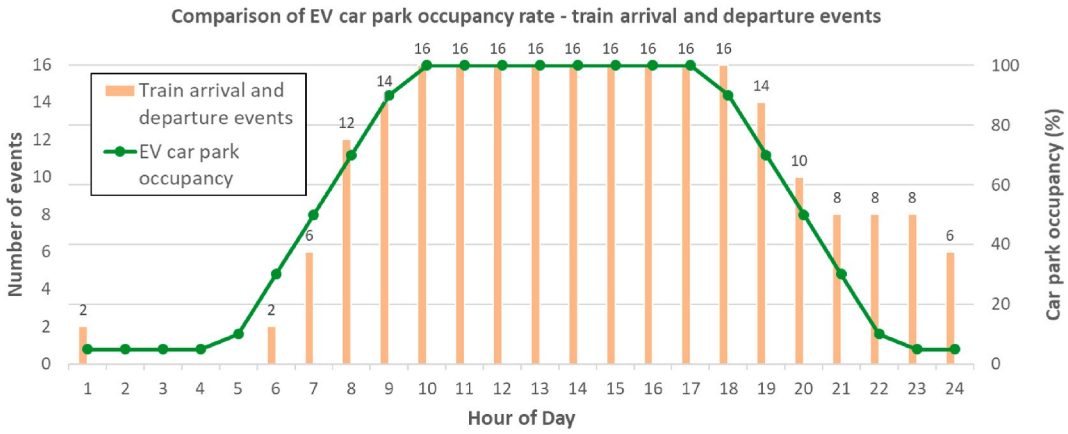

Fig. 3. Assumed car park occupancy rate and number of train arrival/departure events over 24 simulation period.

3. EV population model

The EV population in the proposed V2G system is modelled as a group of parked EVs situated in the same car park, where each EV in the population is assumed to be connected to a bi-directional charger. Non-participation of any connected EVs in V2G operation is not considered. Only the portion of parking spaces in the car park equipped with chargers is considered here (the train station used for this case study has 670 parking spaces available nearby – the scenarios considered in section 4 assume that 50, 75 or 100 of these spaces are equipped with EV chargers respectively). This car park is assumed to have a variable occupancy rate over the simulation period where 0% occupancy represents no connected EVs and 100% represents the all available EV chargers being in use by V2G enabled EVs.

The assumed occupancy rate over the 24 h simulation period is shown in Fig. 3 and is loosely based on data provided by Transport for London (TfL) about car park usage at the London underground (Transport for London TfL, 2010). It is assumed that a car park at a train station is being used similarly (although the example train station is situated in a commuter area rather than an urban environment). The data provided by TfL only covers the ramp-up in occupation in the mornings (6–9 a.m.) and the decrease in the evenings (4–7 p.m.) on a weekday. Thus, further assumptions were needed for a full 24-h car park occupancy rate. Night-time occupancy was assumed to be very low at 5% and day-time occupancy between the morning ramp up and the evening decline was assumed very high at 100%. As seen in Fig. 3, periods of high car park occupancy generally coincide with periods of frequent rail traffic. Defining occupancy using this TfL data is sufficiently representative to define a scenario for modelling, and replacing it with specific data for the car park in question would not alter the conclusions.

For simplicity, all simulated EVs have the same battery pack specifications, mirroring those of the Nissan Leaf (a very common EV model in the UK). Using the specifications of the 2019 Nissan Leaf model, simulated EVs are assumed to have a 40 kWh capacity battery with a charging rate of up to 50 kW (Nissan Motor GB Limited, 2019. It is important to note that this charging rate is only achievable while the battery pack state-of-charge (SOC) is relatively low. The maximum charging rate of each EV depends on the battery pack SOC at the time. Fig. 4 shows the assumed relationship between the maximum charging rate and SOC. This relationship was adapted from the findings in (Bryden et al., 2016). While the maximum discharging rate of the Nissan Leaf battery pack is unknown, the drive train power of this EV is stated as 112 kW. Thus, it is reasonable to assume that the battery pack can be discharged at least at this rate, irrespective of the battery pack SOC. This discharging rate exceeds any of the assumed charging/discharging limits of

the bi-directional EV chargers (also up to 50 kW, see section 4).

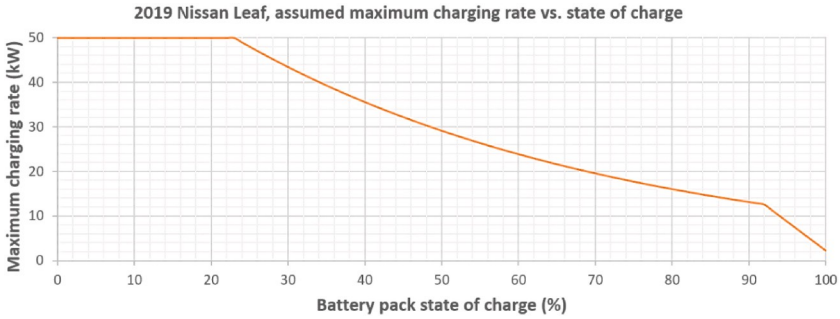

Fig. 4. Assumed maximum charging rate against SOC for simulated EV population.

The V2G aggregator control system used in this work operates in real-time and incorporates all aggregator-to-EV communications (as outlined in (Krueger and Cruden, 2020a)). While V2G communications are not the subject of this particular work, the simulated EV population complies with the existing communication scheme. Each EV is its own instance of an EV simulator algorithm that communicates independently with the aggregator in a master-slave configuration (the EVs only respond to requests from the aggregator). The EV simulator instances are run from a server other than the one handling V2G aggregator control so communication delays are realistically represented.

For this work, the EV population follows the assumed car park occupancy rate in Fig. 3 by adding EVs to the network (i.e. initiating new instances of the EV simulator) until the assumed occupancy rate is reached or by removing EVs from the network whenever the occupancy rate is exceeded. The initial SOC of each simulated EV is random, however, this work uses seeded random number generation so that any two simulations based on the same EV population size use the same seed and thus identical initial SOC values for every EV. To aid the analysis of simulations results, the EV population in each simulation contains three 'control EVs'. These control EVs differ from the 'bulk' of the simulated EV population in that a) connection/disconnection times and initial SOC are always the same and b) changes in SOC over time is monitored and recorded (not true for 'bulk' of EVs due to computational cost):

- EV A – connected from 08:00 to 16:00, initial SOC 50%
- EV B – connected from 09:00 to 17:00, initial SOC 30%
- EV C – connected from 10:00 to 18:00, initial SOC 70%

4. V2G aggregator operation

V2G aggregation within this work assumes that all EVs are connected to identical bi-directional EV chargers (assumed to have the same power rating in both directions) and that both charging and discharging of EVs have an efficiency of 90%. The V2G network is assumed to use the same substation as the rail system and to share its power grid connection (see Fig. 1). It attempts to maintain the power flow from this substation at a constant level – the grid connection limit (a soft constraint rather than a true limit, defined by the proportion of the available power to be managed by the V2G network). At times when the EV population is not able to supply sufficient traction power to the rail system, the power flow from the substation may exceed the grid connection limit to compensate for the deficit. In case of insufficient power absorption from regenerative braking of trains, excess power is assumed to be 'wasted' via heat dissipation

(either through resistor banks or mechanical brakes) and not fed into the grid. In either case, the rail service is not compromised.

The V2G scheduling – the process by which charging/discharging decisions for individual EVs are made – uses the event-based scheduling strategy outlined in (Krueger and Cruden, 2020a). In this strategy, the aggregator determines its response to predictable and repetitive 'events' (here, either the departure or the arrival of a train of known type) separately and shortly before the event begins (10 s prior to departure). For a rail connected system, such predictability does not imply a rail system running without perturbation from the timetable, but instead that the V2G aggregator is aware of train position and timetable information. This predictive scheduling approach minimises delays between changing power demands and the appropriate V2G network response.

EVs on the network are in regular contact with the aggregator to inform about changing battery characteristics (i.e. a changing SOC or the latest maximum charging rate). The aggregator constantly monitors EVs and ranks them in terms of suitability for receiving or supplying power using a dual scoring system (Krueger and Cruden, 2020a). For train departure events (where EVs are discharged to provide traction power) the aggregator prioritises EVs with high battery capacity, high maximum discharging rate and high SOC (each parameter is weighted equally in the scoring system). Such EVs are useful for train departures as they can provide a relatively large quantity of energy relatively quickly (compared to the EV population as a whole). Similarly, for train arrivals (where EVs are charged to absorb power from regenerative braking on the rail system), EVs with high capacity, high maximum charging rate (at the time) and low SOC are prioritised. These EVs can quickly absorb a lot of electric energy (relative to the EV population). All EVs are assumed able to charge or discharge without any hardware or software restrictions (no V2G opt-outs or other EV user control as in (Krueger and Cruden, 2020b)).

The scheduling strategy differentiates between 'in-event' periods (i.e. times of power transfer between the EV population and the rail system) and periods without rail traffic. When no rail traffic occurs the EV population makes use of the shared grid connection for smart charging, where each EV receives a minimum of 1 kW plus a share of the remaining available power corresponding to its ranking (Krueger and Cruden, 2020a). During events, the aggregator assigns EVs sequentially to charge/discharge at the maximum possible rate until the power drawn from the substation matches the pre-determined grid connection limit. The degree to which the V2G network can decouple the power demands of the rail system from the grid connection mainly depends on the following three parameters: the EV population size, the global charging rate limit (the maximum charging/discharging rates per EV as supported by the aggregator) and the anticipated grid connection limit.

4.1. Influence factor 1: size of EV population

The first major factor influencing the performance of the proposed V2G system is the size of the connected EV population (i.e. the number of EVs connected). To investigate this, the 24-h system operation was simulated using EV populations of up to 100, 75 and 50 EVs respectively while the global charging rate limit per EV and the grid connection limit remained constant at 20 kW and 200 kW respectively.

- Scenario 1: 100 EVs
- Scenario 2: 75 EVs
- Scenario 3: 50 EVs

Fig. 5 shows the potential aggregated power output from the V2G network over time in each of the 3 Scenarios. As the global discharging limit of 20 kW is well below the possible power output of any simulated EVs (at no time is any of the EVs fully discharged), the aggregated potential power output of the system is 20 kW times the number of EVs connected at any time. The V2G network is considered capable of fully powering a train departure event (i.e. maximum peak power demand reduction as experienced by the power grid) whenever the power provision potential exceeds the threshold of ~1009 kW (i.e. the peak power demand of the train departure event). As seen in Fig. 5, in scenarios 1 and 2 the system exceeds this threshold from ~06:00 to ~19:00 (a period covering 95 of the 117 daily train departures, ~81%) and ~07:00 to ~18:00 (covering 85 departures, ~73%). Even for scenario 3, a very substantial contribution could be made to the required power (potentially lessening investment needed in sub-station feeds from the grid). Fig. 6 illustrates how the EV population's power provision potential reduces peak power demands as experienced by the substation.

In Fig. 6 (a) the original power demands from train traction power to be met by the substation before considering V2G integration. As expected from the rail system model, the substation experiences a total of 117 short power demand peaks of ~1009 kW from train departures between periods of no power demand. Fig. 6 (b), by contrast, shows reduced power demand peaks when utilising a connected V2G network under the conditions in scenario 2 (chosen as the 'middle ground' scenario). It can be seen that, apart from a minor peak of ~340 kW in the morning (where not enough EVs were yet connected to fully support the first train departure), peaks throughout most of the day (before ~19:00) were quasi eliminated (instead a constant 200 kW were drawn for both EV charging and train traction power). However, in the later hours of the day, the V2G network can no longer fully support traction power and peaks are increasing over time until nearly reaching a megawatt (~949 kW in the final power peak). This points towards the dependence of the proposed system on a sufficient EV population for peak power reduction. While a V2G network with an EV population as modelled in this work is insufficient to eliminate all power demand peaks, temporary peak reduction still greatly benefits the local power grid, reducing the demand for other grid balancing measures.

Fig. 7 shows the V2G network's potential for receiving power over time (i.e. the sum of all EVs maximum charging rate at any point in time, limited to the global charging limit of 20 kW). For each EV the maximum charging power it can receive is dependent on its current SOC as per Fig. 4 (and may fall way short of 20 kW) so this is not a simple reproduction of Fig. 5. For the V2G network to be capable of fully absorbing power from regenerative braking on the rail system, the aggregated power absorption potential has to exceed the threshold of ~1109 kW (i.e. the peak of output of the rail system during a train arrival event). As seen in Fig. 7, this threshold is not reached at any point in scenario 3 (EV population up to 50 EVs) and only during short periods during scenario 2 (up to 75 EVs). Only in scenario 1 (up to 100 EVs) is the V2G network capable of fully absorbing regenerative braking power for an extended period (~7:00 to ~18:00, covering 85 of the 117 train arrivals, ~73%). The other cases demonstrate that a significant contribution can be made to storing regenerated energy even when the car park is less fully occupied.

Comparing Figs. 5 and 7 it should be noted that whenever the power absorption potential of an EV population exceeds the threshold to fully absorb power from a train's regenerative braking, the power provision potential also exceeds the threshold for fully providing traction power. Recalling that 1) the regenerative braking threshold is of a larger magnitude than the traction power threshold and that

2) for each EV the maximum discharging rate is always equal or greater than the maximum charging rate, it follows that, within this work, any EV population capable of fully absorbing regenerative braking energy from an arrival event is also capable of fully providing traction power for a departure event of the same train. As complex events such as simultaneous arrivals and departures by multiple trains are not considered here the analysis below will exclude the power

provision potential of EV populations.

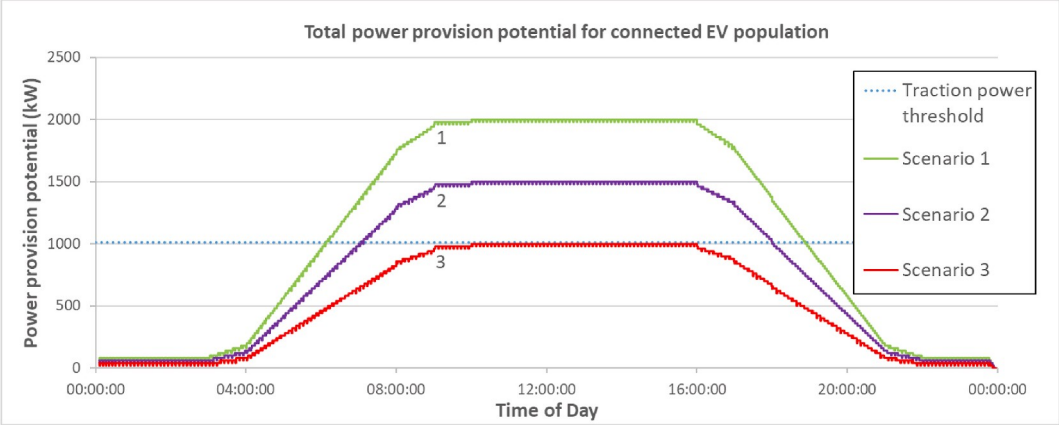

Fig. 5. Total power provision potential of EV populations of varying size over 24 h.

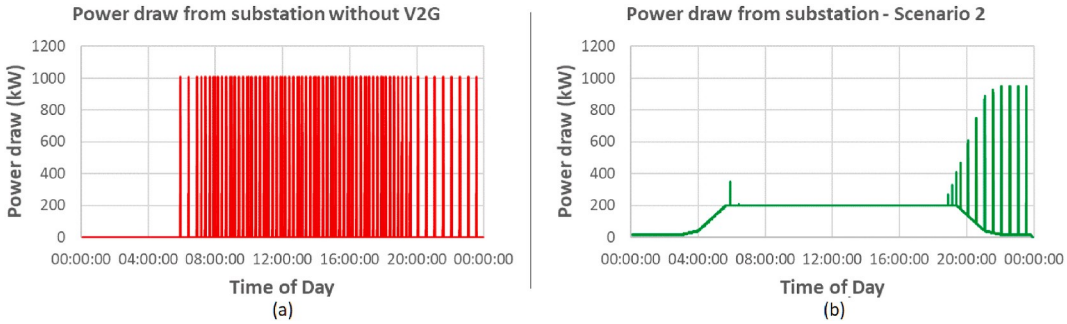

Fig. 6. (a) Power draw from substation for rail system traction power without connected V2G network over 24 h; (b) Power draw from substation for the rail system and EV population power demands with connected V2G network over 24 h (scenario 2).

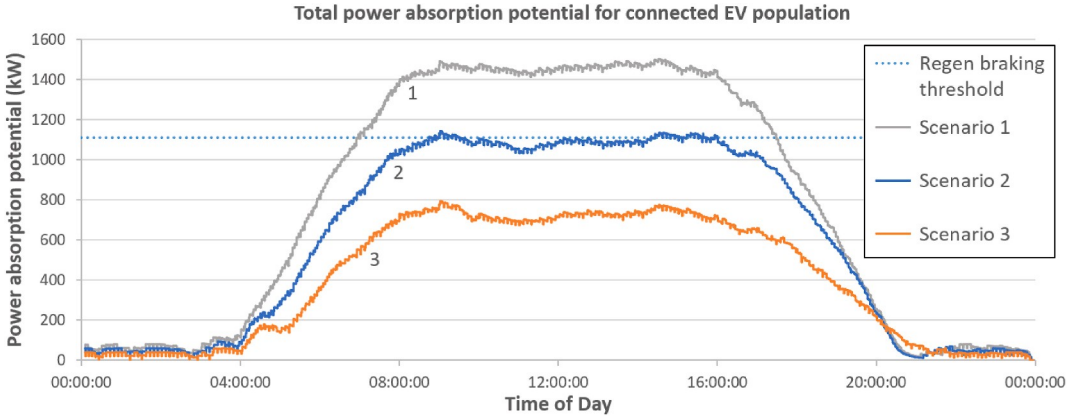

Fig. 7. Total power absorption potential of EV populations of varying size over 24 h.

After considering the V2G network's effectiveness in decoupling the electric rail system and the power grid, its ability to charge individual EVs over time needs to be analysed. Fig. 8 shows how the SOC of the three control EVs develops in each of the three scenarios. Table 1 below shows the final SOC values for each control EV. In any of the three

scenarios, each control EV significantly gained in SOC. As expected, given that the grid connection limit was fixed at 200 kW for all three scenarios (limiting how much power can be shared between EVs during smart charging periods), the SOC gains per EV are higher at lower EV population sizes. While only the control EVs are shown, the observed gain in SOC is indicative of the behaviour in the whole EV population, based on the underlying scheduling rules (Krueger and Cruden, 2020a).

4.2. Influence factor 2: maximum EV charging rates

The next factor influencing system performance is the maximum charging rate available to connected EVs. Each EV has an individual maximum charging rate at any given time (depending mainly on its battery SOC, see Fig. 4), but is also subject to system-wide (i.e. 'global') restrictions, particularly the maximum charging (and discharging) rates supported by the bi-directional chargers each EV is connected to. In this analysis, this system-wide constraint is assumed to be constant, bi-directional (maximum charging rate and maximum discharging rate have the same magnitude) and equal for each EV (i.e. each EV is connected to identical bi-directional chargers). This factor is referred to as the *global charging rate limit* (per EV). Similar to the previous analysis, the 24-h system operation was simulated while varying the global charging rate limit between 50, 35 and 20 kW respectively. The EV population size was 75 EVs and the grid connection limit was 200 kW for each simulation.

- Scenario 1: 50 kW global charging rate limit
- Scenario 2: 35 kW global charging rate limit
- Scenario 3: 20 kW global charging rate limit

As seen in Fig. 9, the difference in power absorption potential between scenarios 1 and 2 is fairly insignificant. This is due to the maximum charging rates of individual EVs dropping below the global charging rate limit as SOC increases (i.e. EVs can only utilise higher global limits while the SOC is low). The power absorption potential in scenario 3 is clearly lower and only meets the threshold sporadically. However, the impact of the global charging limit on the power absorption potential appears to be only moderate suggesting that even lower-end charging hardware may be sufficient for this V2G application.

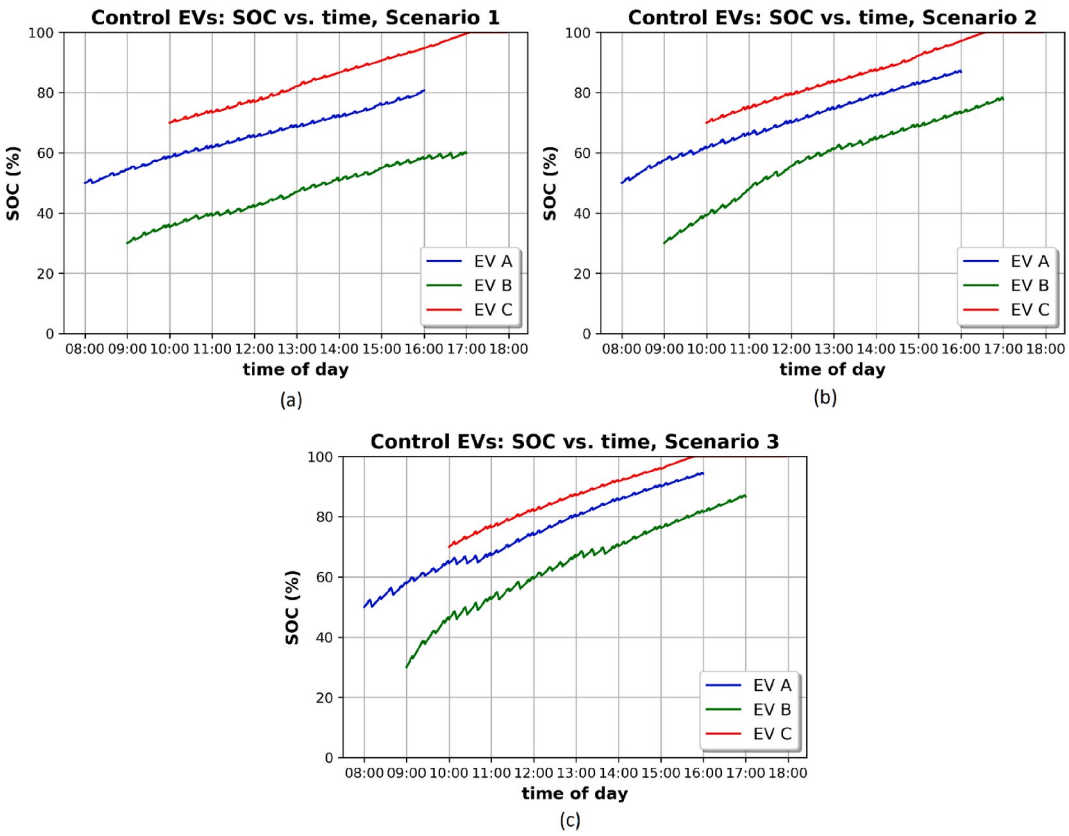

Fig. 8. Changes in SOC over time of the three control EVs within EV populations of varying size.

Table 1: Comparison of Control EV battery pack SOC at departure time for EV populations of varying sizes.

Control EV	SOC at departure (Scenario 1)	SOC at departure (Scenario 2)	SOC at departure (Scenario 3)
EV A	81%	87%	93%
EV B	60%	78%	86%
EV C	100% (at ~ 17:00)	100% (at ~ 16:30)	100% (at ~ 15:45)

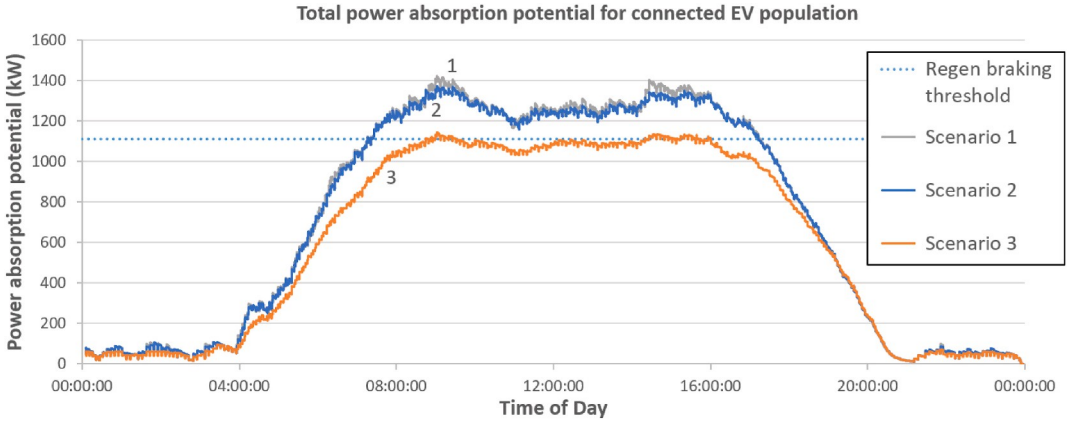

Fig. 9. Total power absorption potential of the connected EV population with varying global charging limits over 24 h.

Analogous to the previous discussion, Fig. 10 shows the changes in SOC over time and Table 2 shows the final SOC for the three control EVs. Comparing the three scenarios, it can be seen that changing the global charging rate limit had very little impact on the control EVs. This can be attributed to the short duration of train arrival and departure events – EV charging and discharging rates approaching the global limit only occur close to peak power regeneration or peak power demand on the rail system. During periods of no rail traffic (nearly 80% of the day) EV charging rates are typically well below the global limit.

4.3. Influence factor 3: grid connection limit

The last factor influencing system performance to be examined in this work is the power made available to the whole system (rail and EVs) via a shared grid connection. Here, the 24-h system operation was simulated several times while varying the grid connection limit (i.e. the soft constraint on the proportion of power available from the substation managed by the V2G network) between 200, 300, 400 and 500 kW respectively. EV population size was kept constant between simulations at 100 EVs and the global charging limit per EV was set to 20 kW.

- Scenario 1: 200 kW grid connection limit
- Scenario 2: 300 kW grid connection limit
- Scenario 3: 400 kW grid connection limit
- Scenario 4: 500 kW grid connection limit

As can be seen in Fig. 11, increasing the grid connection limit significantly hampers the ability of the aggregated EV population to absorb power from the rail system. It should be noted that this impact on the power absorption potential is more pronounced in the afternoon/evening than in the early hours of the day. As the rail system's power demand remains unaltered between scenarios, any increases in the power made available to the system leads to increased EV charging rates and thus faster gains in SOC for connected EVs. However, recall from Fig. 4 that the maximum charging rate for individual EVs decreases with SOC. Consequently, the power absorption potential of the aggregated EV population declines not only when some EV batteries are fully charged, but already as they approach higher SOC levels.

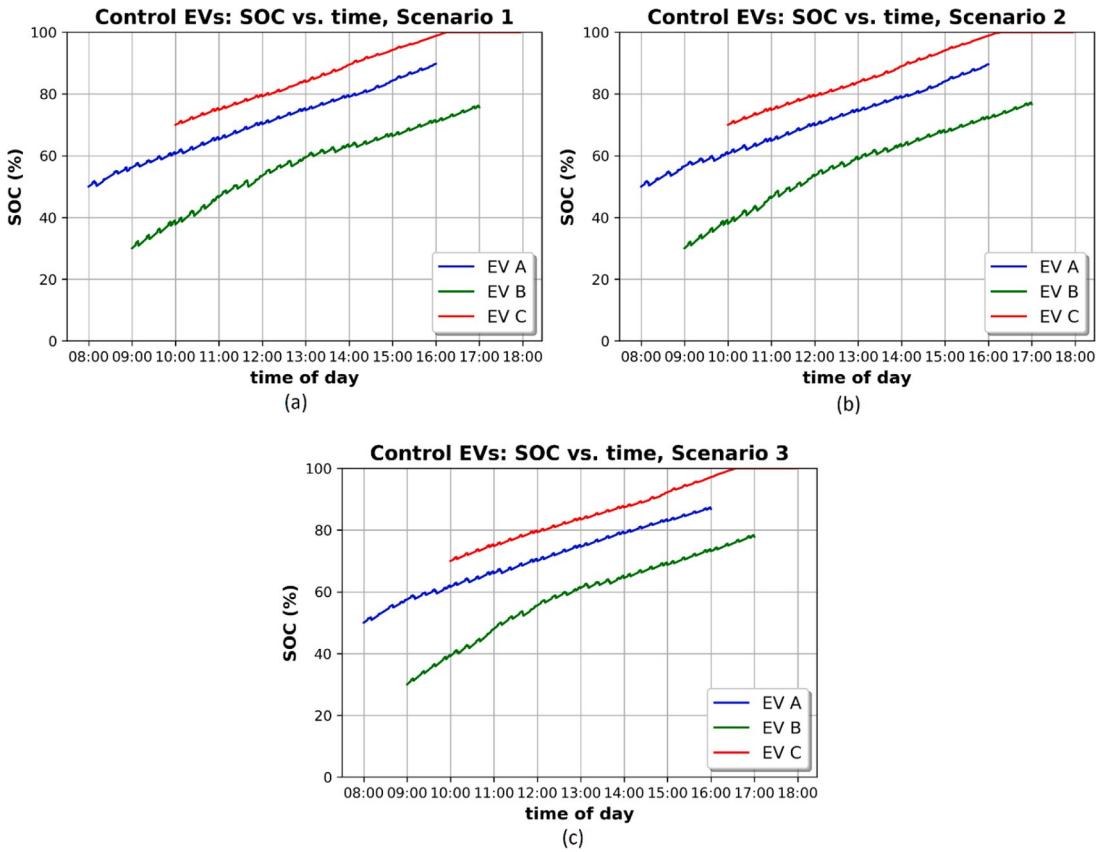

Fig. 10. Changes in SOC over time of the three control EVs within the connected EV population with varying global charging limits over 24 h.

Table 2: Comparison of Control EV battery pack SOC at departure time for different global charging rate limits.

Control EV	SOC at departure (Scenario 1)	SOC at departure (Scenario 2)	SOC at departure (Scenario 3)
EV A	88%	88%	86%
EV B	76%	77%	78%
EV C	100% (at ~ 16:10)	100% (at ~ 16:10)	100% (at ~ 16:30)

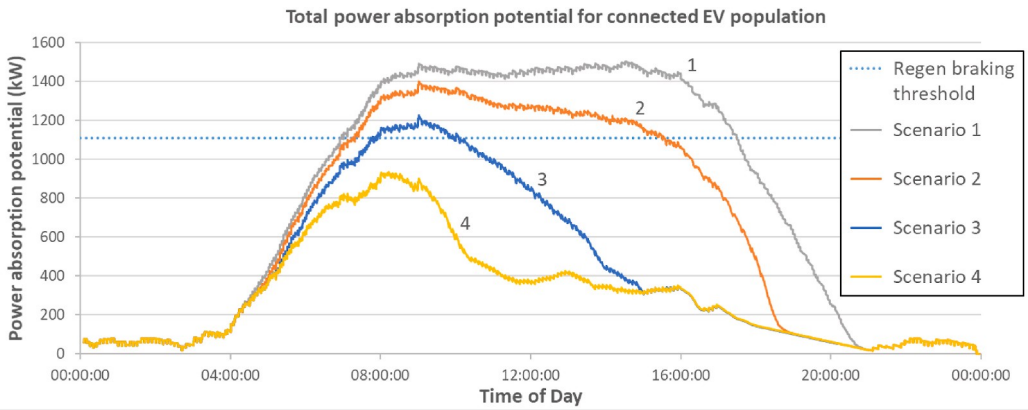

Fig. 11. Total power absorption potential of 100 EVs at varying grid connection limits over 24 h.

These issues stem partially from the simplification within this work to keep the grid connection limit constant throughout the day. More complex scheduling rules that adjust this parameter to the connected EV population may prevent a premature decline in power absorption potential. However, any measures which, in effect, limit EV charging rates need to be considered carefully with regards to EV user acceptance as the V2G network heavily relies on the participation of EV owners/users. Defining charging rate limitations that are acceptable to EV owners should involve social and behavioural science (thus outside the scope of this work).

Examining SOC developments of the control EVs in Fig. 12 as well as Table 3 confirms the previous observations. As expected, the controls EVs are charging faster as the grid connection limit increases. In scenario 4, with the highest simulated grid connection limit of 500 kW, all three control EVs are already fully charged well before midday. While fully charged EVs can no longer absorb power from the rail system's regenerative braking, they are still useful to supply traction power during train departure events.

Table 3: Comparison of Control EV battery pack SOC at departure time for different grid connection limits.

Control EV	SOC at departure (Scenario 1)	SOC at departure (Scenario 2)	SOC at departure (Scenario 3)	SOC at departure (Scenario 4)
EV A	81%	100% (at ~ 15:50)	100% (at ~ 13:00)	100% (at ~ 10:20)
EV B	60%	94%	100% (at ~ 13:40)	100% (at ~ 11:20)
EV C	100% (at ~ 17:10)	100% (at ~ 15:15)	100% (at ~ 13:20)	100% (at ~ 11:15)

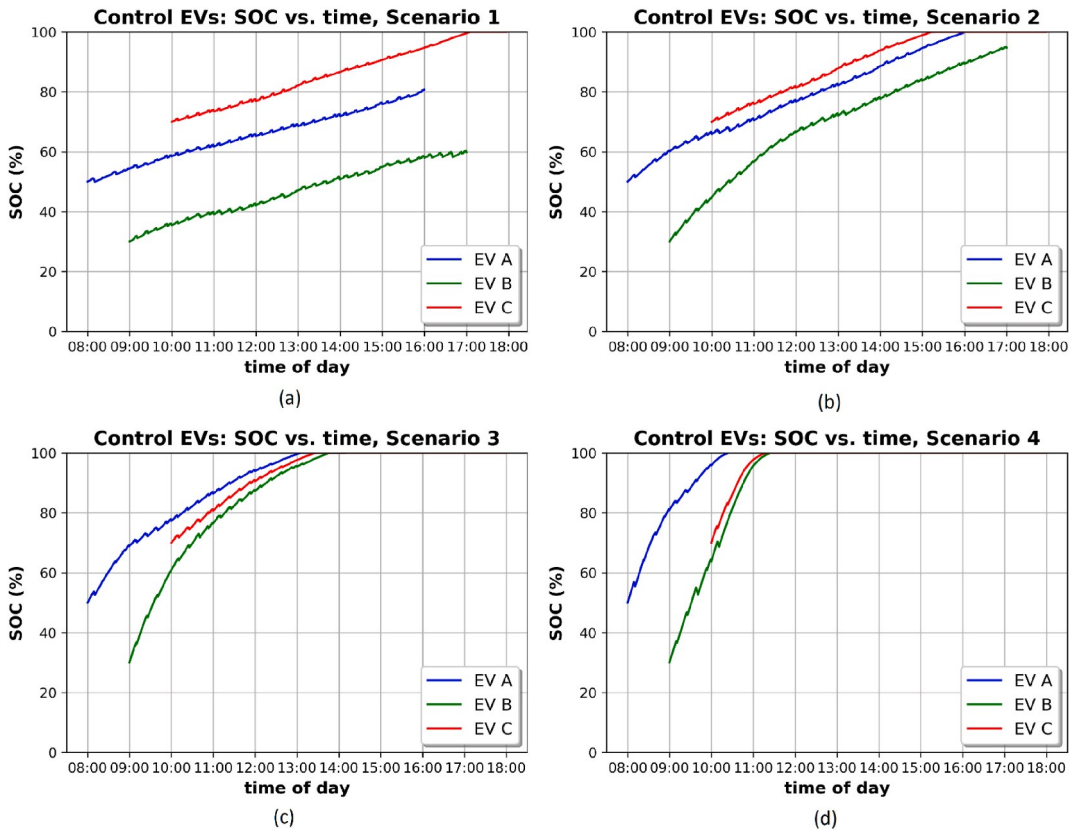

Fig. 12. Changes in SOC over time of the three control EVs within an EV population of 100 EVs at varying grid connection limits over 24 h.

5. Conclusions

In this work, a novel V2G application was proposed in which aggregated parked EVs are charged and discharged to support nearby DC-powered rail systems. Three main factors determining the performance of such a V2G system were identified and examined: the EV population size, the EV charging rates and the power made available to the whole system through the shared power grid connection. While the latter two are controlled design variables for the V2G system, the number of EVs available at any time relies on the participation of EV owners and cannot be fully controlled in a public setting. Thus, determining power ratings of the bi-directional EV chargers and the grid connection limit should follow reasonable estimates of the available EV population size.

Unsurprisingly, the V2G network performs better with larger EV populations although limited availability of EVs in the early and late hours of the day significantly hampers system effectiveness regardless. It was found that individual EV charging rates, in particular, the diminishing maximum charging rates as SOC increases, are more significant than the charging rate limits of the bi- directional chargers (as the V2G network's aggregate power absorption potential, determining its ability to absorb power from the rail system's regenerative braking decreases as EVs are charging). Therefore, having enough EVs with low SOC is more beneficial than highly rated EV chargers.

The power made available to the V2G network via the shared grid connection was found to be a very delicate issue as relatively minor adjustments can cripple the V2G system if EVs charge 'too quickly' to support regenerative braking. The findings point to further work required on optimising management of EV charging in multi-model transport if the desirable benefits of power and energy use reduction are to be realised. Ideally, more sophisticated scheduling algorithms should be used that take information on anticipated EV usage into account (Krueger and Cruden, 2020b). In doing so, the aggregator can ensure sufficient charging of individual EVs (i.e. sufficient charge for planned journeys) while also preserving parts of the EV population with available battery capacity.

The network's power provision potential (determining its ability to provide traction power for train acceleration) is not affected by rapid EV charging - thus maintaining significant peak power reduction as long as enough EVs are connected. However, a permanent high-level reduction of power demand peaks throughout the day could not be achieved with a variable EV population as modelled. To facilitate reliable peak power demand reduction for all daily rail traffic (which might allow for lower-rated power grid connections for rail electrification projects) the V2G network may be reconfigured as part of a hybrid energy storage solution. In this approach, the connected EV population could be accompanied by trackside batteries, flywheels, or other energy storage technologies.

Acknowledgements

The authors would like to acknowledge the support of the Engineering and Physical Sciences Research Council (EPSRC) Centre for Doctoral Training in "Energy Storage and Its Applications" (EP/L016818/1) and the "Transenergy – Road to Rail Energy Exchange (R2REE)" (EP/N022289/1) projects.

References

Bryden, T., Cruden, A., Hilton, G., Dimitrov, B., Ponce de Leo´n, C., Mortimer, A., 2016. Off-vehicle energy store selection for high rate EV charging station. In: 6th Hybrid and Electric Vehicles Conference (HEVC 2016), London, pp. 1–9. https://doi.org/10.1049/cp.2016.0986.

Ceraolo, M., Lutzemberger, G., Meli, E., Pugi, L., Rindi, A., Pancari, G., 2018. Energy storage systems to exploit regenerative braking in dc railway systems: different approaches to improve efficiency of modern highspeed trains. Journal of Energy Storage 16, 269–279. https://doi.org/10.1016/j.est.2018.01.017.

Darcovich, K., Recoskie, S., Ribberink, H., Pincet, F., Foissac, A., 2017. Effect on battery life of vehicle-to-home electric power provision under Canadian residential electrical demand. Appl. Therm. Eng. 114, 1515–1522. https://doi.org/10.1016/j.applthermaleng.2016.07.002. ISSN 1359-4311.

Department for Business, Energy & Industrial Strategy, 2019. Sub-national Electricity and Gas Consumption Summary Report 2018. online resource. https://www. gov.uk/government/collections/sub-national-electricity-consumption-data. (Accessed 22 April 2020).

EA technology, 2018. My Electric Avenue - Summary Report. online resource. http://myelectricavenue.info/sites/default/files/Summary%20report.pdf. (Accessed 21 June 2020).

Transport for London (TfL), 2010. Car Park Usage at London Underground. TfL publications. http://content.tfl.gov.uk/car-park-usage-at-london-underground-report. pdf. (Accessed 8 September 2020).

D. Fletcher, R. Harrison, S. Nallaperuma, "TransEnergy – a tool for energy storage optimization, peak power and energy consumption reduction in DC electric railway systems", Journal of Energy Storage, Volume 30, 2020, doi: 10.1016/j.est.2020.101425.

Freeman, G., Drennen, T., White, A., 2017. Can parked cars and carbon taxes create a profit? The economics of vehicle-to-grid energy storage for peak reduction. Energy Pol. 106, 183–190. https://doi.org/10.1016/j.enpol.2017.03.052. ISSN 0301-4215.

Grenier, A., Page, S., 2012. The impact of electrified transport on local grid infrastructure: a comparison between electric cars and light rail. Energy Pol. 49, 355–364. https://doi.org/10.1016/j.enpol.2012.06.033.

Habib, S., Kamran, M., Rashid, U., 2015. Impact analysis of vehicle-to-grid technology and charging strategies of electric vehicles on distribution networks – a review. J. Power Sources 277, 205–214. https://doi.org/10.1016/j.jpowsour.2014.12.020.

International Energy Agency, 2019a. Energy Efficiency Indicators 2019. IEA publications, pp. 5–8. https://www.iea.org/reports/energy-efficiency-indicators-2019. (Accessed 3 May 2020).

International Energy Agency, 2019b. Global EV Outlook 2019. IEA publications, pp. 9–10. https://www.iea.org/reports/global-ev-outlook-2019. (Accessed 3 May 2020).

Kim, J., Suharto, Y., Daim, T., 2017. Evaluation of electrical energy storage (EES) technologies for renewable energy: a case from the US pacific Northwest. Journal of Energy Storage 11, 25–54. https://doi.org/10.1016/j.est.2017.01.003.

Krueger, H., Cruden, A., 2020a. Multi-layer event-based vehicle-to-grid (V2G) scheduling with short term predictive capability within a modular aggregator control structure. IEEE Trans. Veh. Technol. 69 (5), 4727–4739. https://doi.org/10.1109/TVT.2020.2976035.

Krueger, H., Cruden, A., 2020b. Integration of electric vehicle user charging preferences into Vehicle-to-Grid aggregator controls. Energy Rep. 6, 86–95. https://doi. org/10.1016/j.egyr.2020.02.031, 2020.

Li, X., Castellanos, S., Maassen, A., 2018. Emerging trends and innovations for electric bus adoption—a comparative case study of contracting and financing of 22 cities in the Americas, Asia-Pacific, and Europe. Res. Transport. Econ. 69, 470–481. https://doi.org/10.1016/j.retrec.2018.06.016.

Lin, F., Liu, S., Yang, Z., Zhao, Y., Yang, Z., Sun, H., 2016. Multi-train energy saving for maximum usage of regenerative energy by dwell time optimization in urban rail transit using genetic algorithm. Energies 9 (3), 208. https://doi.org/10.3390/en9030208.

Merseyrail, 2019. Train Times Wirral Line. online resource. https://www.merseyrail.org/media/1295978/wirral-line-from-15th-december-2019-to-16th-may-2020- website.pdf. (Accessed 17 March 2020).

Mwambeleko, J., Kulworawanichpong, T., 2017. Battery electric multiple units to replace diesel commuter trains serving short and idle routes. Journal of Energy Storage 11, 7–15. https://doi.org/10.1016/j.est.2017.01.004.

Nissan Motor (GB) Limited, 2019. Nissan Leaf - Technology & Performance. product brochure. https://www-europe.nissan-cdn.net/content/dam/Nissan/gb/ brochures/Vehicles/Nissan_Leaf_UK.pdf. (Accessed 8 September 2020).

Pavi´c, I., Capuder, T., Kuzle, I., 2015. Value of flexible electric vehicles in providing spinning reserve services. Appl. Energy 157, 60–74. https://doi.org/10.1016/j.apenergy.2015.07.070.

Peng, C., Zou, J., Lian, L., Li, L., 2017. An optimal dispatching strategy for V2G aggregator participating in supplementary frequency regulation considering EV driving demand and aggregator's benefits. Appl. Energy 190, 591–599. https://doi.org/10.1016/j.apenergy.2016.12.065.

Stewart, E., Weston, P., Hillmansen, S., Roberts, C., 2011. The Merseyrail Energy Monitoring Project. 9th World Congress on Railway Research. http://www.railway- research.org/IMG/pdf/a4_weston_paul.pdf. (Accessed 3 September 2019).

Tomi´c, J., Kempton, W., 2007. Using fleets of electric-drive vehicles for grid support. J. Power Sources 168 (2), 459–468. https://doi.org/10.1016/j.jpowsour.2007.03.010.